MANIPULATION OF HEAT FLUX PATHS IN THERMO-ELASTICALLY DAMPED RESONATORS FOR Q OPTIMIZATION

Dustin D. Gerrard, Janna Rodriguez, Lizmarie Comenencia Ortiz, Saurabh A. Chandorkar, Ian B. Flader, Yunhan Chen, Dongsuk D. Shin, and Thomas W. Kenny
Stanford University, Stanford, California, USA

ABSTRACT

We demonstrate how to identify regions of major thermo-elastic dissipation (TED) in MEMS resonators and reduce this energy loss by modifying the device geometry. To demonstrate this, various geometries of a disk resonating gyroscope (DRG) are used. Devices are fabricated and tested to show that the TED-limited quality factor (Q) can indeed be increased using geometric manipulation, as predicted by simulation.

INTRODUCTION

Thermo-elastic Dissipation

Energy loss through TED is a well understood process that occurs when heat irreversibly flows across the temperature gradient caused by elastic deformation in resonating structures. The coefficient of thermal expansion (α) plays a major role in this process as regions of a resonator in compression increase in temperature and regions in tension cool down (Fig. 1, left). At low frequencies the vibrations are isothermal and at high frequencies they are adiabatic [1, 2, 3]. Energy loss through TED reaches a maximum (minimum Q_{TED}) at intermediate frequencies when the mechanical time constant and thermal time constant are equivalent (Fig. 2). The relationship between Q_{TED} and resonant frequency (f) of a clamped-clamped beam is known analytically (Fig. 2) [1, 2, 3].

It has been shown that placing slots in a clamped-clamped beam can disrupt the flow of heat and increase Q by a factor of 4 [4]. Figure 1 illustrates that a slot placed in the central axis of a beam impedes the flow of heat (Fig.1 also shows heat flux which will be discussed in the Geometry Design Optimization section).

Many MEMS resonators, such as the DRG, have significantly more complicated geometry than a simple beam. Q_{TED} in these more complex devices can be estimated with heat mode analysis [5]. For all such devices, TED can be reduced by splitting the mechanical and thermal time constants.

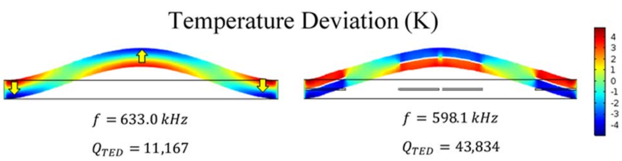

Figure 1: The path of heat conduction from hot to cold regions in a solid resonating clamped-clamped beam (left) is impeded by placing slots in the beam (right). Yellow arrows indicate the path of heat flow.

Disk Resonating Gyroscope

In this paper we focus on DRGs [6] whose f-Q relationship is not known analytically due to the complexity of the disk geometry. Using COMSOL to

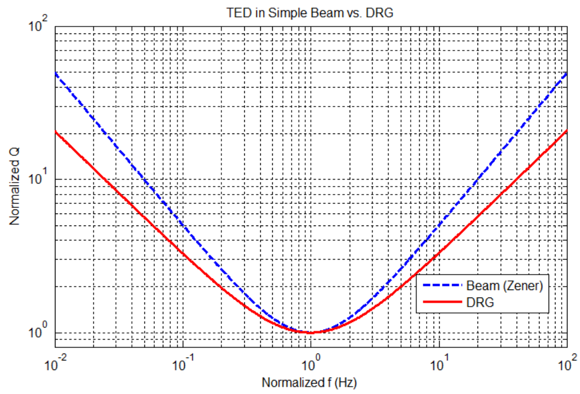

Beam (Zener)

$$Q_{TED} = \frac{C_P \rho}{E\alpha^2 T_0} \cdot \frac{1 + (\omega\tau)^2}{(\omega\tau)}$$

DRG (simplified model)

$$Q_{TED} = c_3 \frac{C_P \rho}{E\alpha^2 T_0} \cdot \frac{c_2 + (\omega\tau)^{c_1}}{(\omega\tau)^{(\frac{c_1}{2})}}$$

Figure 2: Normalized Zener curve for simple beams and normalized Q-f curve for parameterized DRG. The Equations for these curves are given. The coefficients for Q_{TED} are provided in Fig 2. And tau is the mechanical time constant. The value of c1 is less than 2 for all DRGs. The f-Q curve for the DRG is determined from COMSOL simulations whereas the beam (Zener) is analytic.

perform hundreds of parametric simulations we obtain a Zener-like f-Q relationship as shown in Figure 2. The curvature of the f-Q curve is less than that of the Zener curve and is directly dependent on the ring width (r_w). Fabricated DRGs have been shown to follow this relationship [7].

The DRG is driven electrostatically in the n = 2 wine-glass mode (see Fig. 3) [8]. When rotation occurs about the z-axis energy is coupled via the Coriolis force from the drive mode into the orthogonal sense mode. The quality factor is a critical performance metric for device operation [9], and thus we seek obtain a higher Q [10, 11].

It has been shown that TED is a major loss mechanism in DRGs, and anchor loss, and air damping also are major energy loss mechanisms [7]. The total quality factor of the resonator is expressed as the reciprocal sum.

$$\frac{1}{Q_{TOT}} = \frac{1}{Q_{TED}} + \frac{1}{Q_{AIR}} + \frac{1}{Q_{Anchor}} + \cdots \qquad (1)$$

We achieve a higher Q and qualify the relationship between f and Q and experimentally quantify the major energy loss modes.

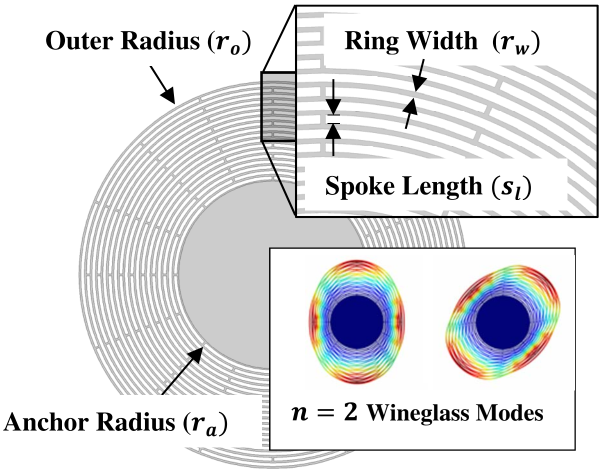

Figure 3: DRG parameters of interest including outer radius, anchor radius, ring width, volume fraction. The DRG operates in the wine-glass mode (n=2).

GEOMETRY DESIGN OPTIMIZATION

Design parameters of the DRG geometry are shown in Figure 3. The spoke length (s_l) is fixed at 1.5 µm in all DRG simulations use for finding the Zener-like f-Q relationship. The ring width is fixed for a single species of DRG (as is the beam width for a beam in the Zener model) and resonant frequency of the device is controlled by varying the number of rings in the DRG. The anchor radius (r_a) is constrained to be exactly half of the outer radius (r_o). Each DRG has 16 spokes alternating between rings (Fig. 3) [6].

To decrease the TED in a resonator, the total heat flux must be reduced. This can be accomplished by reducing the thermal conductance across temperature gradients by engineering the mechanical and thermal time constants.

The thermal conductance of a prismatic solid is defined as

$$P_{COND} = \frac{\kappa A}{L} \quad (2)$$

where A is cross-sectional area, L is length, and κ is thermal conductivity. Thus, conductance in a fixed medium can be reduced by decreasing the cross-sectional area or increasing the length.

Heat dissipation regions can be identified in the DRG by plotting heat flux as was shown in Figure 4 for beams [4]. Heat flux is calculated in units of W/m^3 as the absolute value of temperature differential multiplied by thermal conductivity. This value is integrated over one resonance cycle and is expressed as the following.

$$\oint \kappa\sqrt{dT_x^2 + dT_y^2 + dT_z^2}\,dt \quad (3)$$

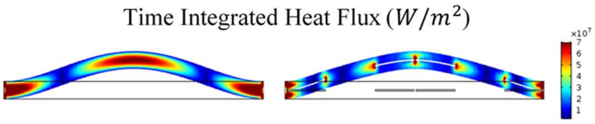

Figure 4: Heat flux in the solid beam is greatest along its central axis at the middle and ends. When the beam is slotted heat flux is concentrated at the ends of the slots. Heat flux is calculated using equation 3.

The terms dT_i correspond to the spatial temperature gradient in the i axis (i.e. $dT_i = \partial T/\partial i$).

An eigenfrequency study is performed on the DRG using a 3D model in COMSOL. To visualize the fine detail of temperature deviation and heat flux in the DRG the mesh is greatly refined, which is only computationally feasible in a small portion of the device. Accurate results are achieved by utilizing the inherent symmetry of the DRG, and refining the hexahedral mesh solely in a rectangular region of interest, as shown in Figure 5. Temperature deviation of the 45º wineglass mode is plotted, and it can be seen that the rings of the DRG alternatively heat up and cool down. Yellow arrows indicate the path of heat flow; major heat flow paths are through the spokes and across the rings where they meet the spokes. The heat flux is also calculated using equation 3 and plotted in the bottom of Figure 5. Red regions represent large and blue regions represent small heat flux. The greatest concentration of heat flow is seen to be through the edges of the spokes and is thus a region of major entropy generation from TED. The understanding of heat flux enables us to directly make basic geometric changes to improve Q, as demonstrated with the beam [4].

The DRG geometry is manipulated to decrease the thermal conductance (P_{COND}) by increasing the length of

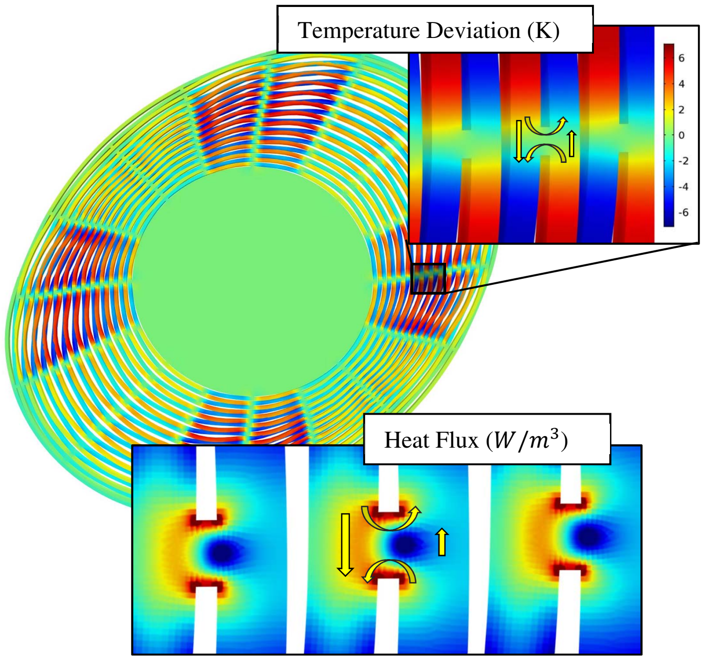

$f = 175\ kHz$ $N = 25$ $r_w = 5.224\ \mu m$
$Q = 114\ k$ $s_l = 1.77\ \mu m$ $r_o = 406\ \mu m$

Figure 5: Wineglass mode of a DRG with ring width of 6µm minus over-etch. (top) Temperature deviation of the full device and zoomed-in region. Units are in Kelvin. (bottom) Time integrated heat flux through spokes of the DRG. Blue domains have low heat flux and red regions have high heat flux. Yellow arrows indicate the path of heat flow.

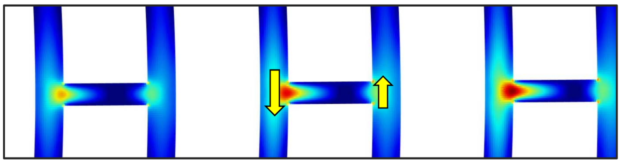

Figure 6: Zoomed-in view of DRG rings. By increasing the spoke length and decreasing the spoke width, a major heat flow path is diminished thus raising Q. Yellow arrows indicate the path of heat flow. This does not always increase the Q but we see qualitatively that less heat flows through the spokes when compared with Figure 5. This is the basis for optimizing our DRGs.

the heat flux path (i.e. the spoke). Figure 6 illustrates that the heat flux through the spokes is significantly reduced when they are made longer. Simulated Q_{TED} is seen to be much higher in this device than the baseline device, despite having the same frequency. For all designs, the outer radius of the disk (r_o) is always fixed to be exactly twice that of the DRG anchor radius ($r_o = 2 * r_a$). The size of the anchor has negligible impact on TED simulation.

FABRICATION AND TESTING

Several sets of DRGs are fabricated each consisting of ring widths 3µm, 6µm, and 9 µm to obtain a baseline f-Q curve. These standard DRGs have 1 µm spoke length and 1.5 µm gap between device and electrodes. Additional DRGs with 3µm ring width and longer spokes (for higher Q). Devices are fabricated on a 40 µm device layer SOI using an epitaxially, vacuum encapsulated "epi-seal" process [12], and a modified version of this process enables long spokes to be fabricated [13]. DRGs with large outer radius (r_o) suffered from process stiction failures. An SEM image of a device is shown in Figure 7. Testing is done using a ring down setup as shown in Figure 7. Devices are vented with focused ion beam milling, allowing data to be collected over a wide range of pressures and temperatures.

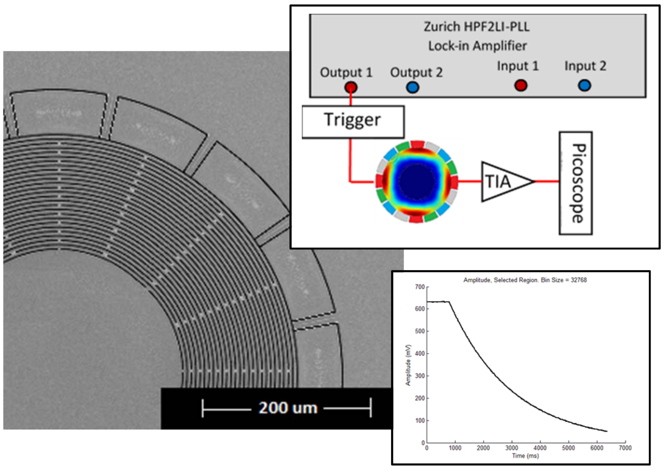

Figure 7: (left) SEM images of DRG. (top right) Lock-in amplifier setup for testing. (bottom right) Ringdown data.

RESULTS AND DISCUSSION

Figure 8 shows simulated f-Q relationships for DRGs of three different ring widths (r_w). The region of standard DRGs able to be fabricated using *episeal* is shaded gray. Experimental data for devices is seen to be in close agreement indicating that they are loss limited by TED [Gerrard]. The discrepancy between simulated Q_{TED} and experimental results is accounted for by air and anchor damping, which affect each DRG design differently.

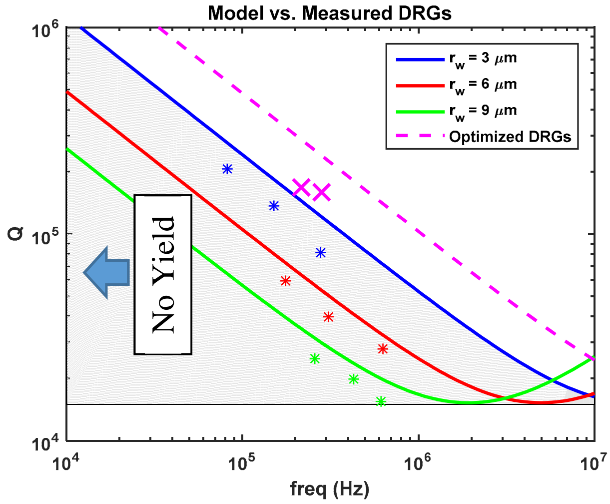

*Figure 8: Parameterized DRG simulations are plotted using lines and measured data is potted using *'s and x's. Optimized DRGs have longer spokes. Colors correspond to geometry type. The gray region indicates the feasible f-Q of DRG in the standard episeal process with 1.5µm gap size.*

The Q is measured for two vented devices and plotted as a function of pressure in Figure 9. The native pressure inside *episeal* devices is approximately 0.1 Pa.

Measurements of Q are taken from -40□ to 85□ and

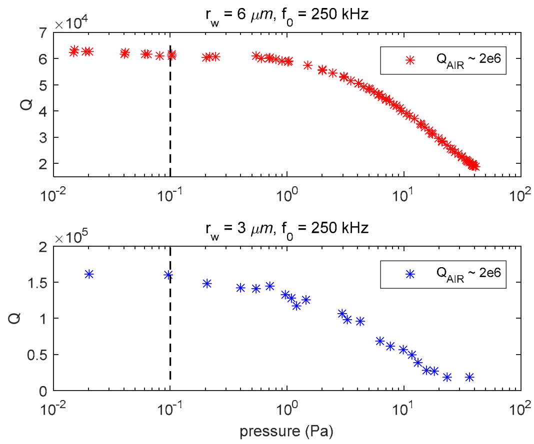

Figure 9: Experimental Q for vented DRG at different pressures. Pressure inside episeal devices is around 0.1 Pa. Air loss has low impact for 6µm ring device.

compared with a simulation of TED (see Fig. 6). From this we extract the Q of all other modes. The discrepancy between the TED model predictions and our experimental results reveals the presence of additional dissipation mechanisms, particularly in the devices with the least thermo-elastic dissipation.

CONCLUSION

The Q of a resonant beams and DRGs can be increased

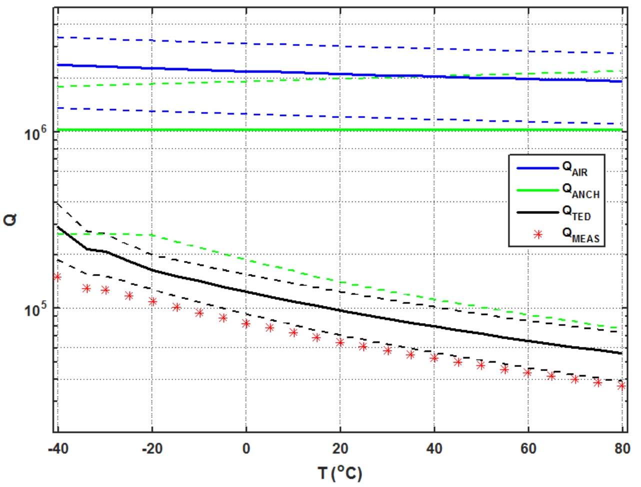

Figure 10: Measured Q of a 6 um ring width DRG and estimated loss modes. Air loss is based on vented devices and TED is from simulation. Dotted lines indicate range of uncertainty. There is large uncertainty in anchor loss.

via manipulations to the geometry. For DRGs, major heat flux occurs through the spokes and lengthening them increases the Q. This modification, however, comes at a cost to the gyroscope as it has lower mass density. A better design would increase Q without sacrificing mass.

This process of identifying heat flux enables a MEMS designer to identify regions of major heat flux, and allows for a straight-forward method of improving the device performance through geometric modification. The correlation between Q and f for DRGs shows a feasible design space. Optimization can use this as a way of determining how much better the designs are. MEMS designers can easily use FEM software to identify regions of major heat flux allowing for an intuitive way of manipulating geometry to increase Q.

This methodology effectively allows for independent modification of the thermal time constant and mechanical time constant which can significantly increase Q. This can be used to enhance the Q in other TED-limited devices.

ACKNOWLEDGEMENTS

This work was supported by the Defense Advanced Research Projects Agency (DARPA) Precision Navigation and Timing program (PNT) managed by Dr. Andrei Shkel and Dr. Robert Lutwak under contract # N66001-12-1-4260. The fabrication work was performed at the Stanford Nanofabrication Facility (SNF) which was supported by National Science Foundation through the NNIN under Grant ECS- 9731293.

The author would also like to thank the National Defense Science and Engineering Graduate (NDSEG) program and A. Dorian Challoner.

REFERENCES

[1] C. Zener. "Internal friction in solids. I. Theory of internal friction in reeds." Physical review 52.3 (1937): 230.

[2] C. Zener. "Internal friction in solids II. General theory of thermoelastic internal friction." Physical Review 53.1 (1938): 90.

[3] C. Zener, W. Otis, and R. Nuckolls. "Internal friction in solids III. Experimental demonstration of thermoelastic internal friction." *Physical Review* 53.1 (1938): 100.

[4] R. N. Candler, et al. "Impact of geometry on thermoelastic dissipation in micromechanical resonant beams." Journal of Microelectromechanical Systems, 15.4 (2006): 927-934.

[5] S. A. Chandorkar, R. N. Candler, A. Duwel, R. Melamud, M. Agarwal, K. E. Goodson, T. W. Kenny. "Multimode thermoelastic dissipation." Journal of Applied Physics 105.4 (2009): 043505.

[6] A. D. Challoner and K. V. Shcheglov, "Isolated planar gyroscope with internal radial sensing and actuation," 7,040,163, 2006.

[7] D. D. Gerrard, C.H. Ahn, I. B. Flader, Y. Chen, E. J. Ng, Y. Yang, & T. W. Kenny (2016, January). Q-factor optimization in disk resonator gyroscopes via geometric parameterization. In *2016 IEEE 29th International Conference on Micro Electro Mechanical Systems (MEMS)* (pp. 994-997). IEEE.

[8] C.H. Ahn, E. J. Ng, V. A. Hong, J. Huynh, T. W. Kenny, and S. Wang, "Oxide-coated polysilicon disk resonator gyroscope (DRG) within the wafer-scale encapsulation process," 2015 IEEE International Symposium on Inertial Sensors and Systems (ISISS) Proceedings, pp. 1-2, Mar 2015.

[9] C. H. Ahn, S. Nitzan, E. J. Ng, V. A. Hong, Y .Yang, T. Kimbrell, ... & T. W. Kenny, T. W. (2014). Encapsulated high frequency (235 kHz), high-Q (100 k) disk resonator gyroscope with electrostatic parametric pump. *Applied Physics Letters*, *105*(24), 243504.

[10] R. Mirjalili, et al. "Substrate-decoupled silicon disk resonators having degenerate gyroscopic modes with Q in excess of 1-million." Solid-State Sensors, Actuators and Microsystems (TRANSDUCERS), 2015 Transducers-2015 18th International Conference on. IEEE, 2015.

[11] A. Sharma, F. M. Zaman, B. V. Amini, & F. Ayazi (2004, October). A high-Q in-plane SOI tuning fork gyroscope. In *Sensors, 2004. Proceedings of IEEE* (pp. 467-470). IEEE.

[12] A. Partridge, and M. Lutz. "Episeal pressure sensor and method for making an episeal pressure sensor." U.S. Patent No. 6,928,879. 16 Aug. 2005.

[13] Y. Yang, E. J. Ng, Yunhan Chen, I. B. Flader, C. H. Ahn, V. A. Hong, and T. W. Kenny, "A unified epi-seal process for resonators and inertial sensors," 2015 Transducers - 2015 18th International Conference on Solid-State Sensors, Actuators and Microsystems (TRANSDUCERS), pp. 1326-1329, Jun 2015.

CONTACT

*D. D. Gerrard, tel: +1-650-847-0402;
dgerrard@stanford.edu